Case Studies in Construction Materials 20 (2024) e02708

Contents lists available at ScienceDirect

Case Studies in Construction Materials

journal homepage: www.elsevier.com/locate/cscm

Short communication

A new approach for characterizing internal stress of fresh concrete during thermal treatment period

Yu Xiang [a,*], Jionghuang He [b], Guangcheng Long [a], Youjun Xie [a], Jilin Wang [a,*]

[a] School of Civil Engineering, Central South University, Changsha, Hunan 410075, China
[b] Department of Civil and Environmental Engineering, The Hong Kong Polytechnic University, 100872, Hong Kong, China

ARTICLE INFO

Keywords:
Fresh concrete
Thermal treatment
Internal stress
Characterization

ABSTRACT

Addressing the scarcity of research on the residual expansion deformation of steam-cured concrete and its underlying factors, this study introduces a testing apparatus to characterize the internal stress in fresh concrete during the thermal treatment. It explores the impact of water-to-cement ratio (w/c) and paste-to-aggregate ratio (p/a) on internal stress and elucidates the developmental patterns of internal stress in concrete throughout the thermal treatment phase. The key findings are as follows: (i) During the thermal treatment, the internal stress in concrete under constraint is predominantly compressive, exhibiting a rapid increase in the heating stage, followed by a gradual decline in the constant temperature treatment stage, and a continued decrease with a decelerating trend during the cooling stage. (ii) Both w/c and p/c significantly influence internal stress in concrete, and this stress can be enhanced by reducing the initial free water content and augmenting the initial structural strength of the concrete. This paper serves as a valuable foundation and reference for further investigations into the residual expansion deformation of steam-cured concrete.

1. Introduction

The residual expansion deformation of steam-cured concrete refers to the irreversible volumetric expansion experienced by concrete following the completion of a full steam curing process [1]. Fresh concrete, signifying concrete that has just been mixed and is in its initial setting phase, undergoes a certain degree of shrinkage and temperature-related deformation. Additionally, it experiences varying levels of internal expansion pressure, shrinkage stress, and humidity and temperature-induced stresses during the steam curing process. The volumetric deformation process of fresh concrete can be driven, and its internal microstructure will be affected under the combined effect of these complex internal stresses. The existing research results indicate that if the residual expansion deformation is more remarkable [1–3], the pore structure will be coarsened [4–6], the brittleness will increase [7,8], and the mechanical and durability performance of the steam-cured concrete prefabricated components will be more adversely affected [2]. Therefore, in order to reveal the causes of the residual expansion deformation of steam-cured concrete and make the precast components achieve the best performance, it is necessary to grasp the internal stress development changing rules in fresh concrete under the action of non-steady state humidity-and-heat coupling environment.

The dual-ring restraint test studied by Xia and et al. [9] provides insights into conducting a dual-ring test under steam curing conditions. They investigated the early restraining stresses inside the cement mortar using an expansion agent under the dual invar

* Corresponding authors.
E-mail addresses: niesh2013@126.com (Y. Xiang), wjlcsuer@gmail.com (J. Wang).

https://doi.org/10.1016/j.cscm.2023.e02708
Received 3 September 2023; Received in revised form 5 November 2023; Accepted 21 November 2023
Available online 23 November 2023

ring restraint, obtaining annular internal stresses on the contact surface between the cementitious materials and the outside of the inner invar ring. He [10] employed an improved dual steel rings restraint test to examine the cementitious materials with expansion characteristics and the residual stresses generated in the early stage. The test device is shown in Fig. 1. Annular strains can be collected by strain gauges on the inner and outer steel rings after the volume change of the cementitious materials begins during the steam curing process.

Fig. 2 displays the annular strains of steel rings driven by the volume expansion of cement paste during steam curing (2 h of heating, 8 h of constant temperature curing (60 °C), followed by natural cooling), with positive values indicating tensile strains. As observed in Fig. 2, the outer steel ring consistently exhibits tensile deformation, while the inner steel ring displays compressive deformation. Both the outer steel ring and the inner steel rings experience a significant increase in strain with rising temperature, reaching their maximum values during the heating stage, followed by a decrease upon entering the constant temperature curing stage. Finally, they maintain relative stability during the cooling stage. This suggests that the heating stage of the steam curing process is the primary phase responsible for the notable expansion deformation in the cementitious materials.

However, the modified dual steel rings restraint test involved the attachment of multiple sets of resistive strain gauges to the test specimen and its dual steel rings, which were placed in a steam curing chamber for monitoring and curing. During the monitoring process, the authors discovered that the resistive strain gauges, affixed tightly to the dual steel rings using superglue and epoxy resin, exhibited signs of loosening in the humidity-and-heat environment during the heating stage, rendering some of the data unavailable.

Moreover, the resistive strain gauges deformed in tandem with the volume changes of the rings, but their deformation could not be fully restored to their pre-test state after the dual steel rings were cooled to room temperature. Subsequently, when the same resistive strain gauges were used to test the next group of specimens, similar results were often not obtained, and sometimes even yielded significantly different results. Replacing all the resistive strain gauges and re-attaching them to the rings posed challenges as it introduced errors in the positioning due to manual measurements and the characteristics of new gauges themselves, ultimately resulting in unsatisfactory test outcomes.

Considering the aforementioned research limitations, the authors have introduced an integrated testing device and method [11] to quantitatively assess and analyze the internal stress of fresh concrete subjected to thermal conditions. This simulation mirrors the unsteady humidity-and-heat environment experienced during steam curing. The internal stresses of concrete, when subjected to dual steel rings restraint during the thermal treatment period, were tested and computed for various *w/c* and *p/a* ratios. This paper also presents the principles for controlling the internal stress of steam-cured concrete.

2. Experimental device, methodology, and materials

2.1. Test equipment, mould, and sample forming process

In order to characterize the internal stress of fresh concrete during the thermal treatment period, a non-contact dual steel rings test system is designed, as shown in Fig. 3.

It mainly includes test equipment, data acquisition equipment, data processing procedures, and concrete specimens. The inner and outer radii of the inner steel ring are 60 mm and 75 mm, respectively, while the inner and outer radii of the outer steel ring are 185 mm and 200 mm, respectively. The height of the dual steel rings is 75 mm. Due to the limited deformation and cost-effectiveness of 304 alloy steel within the range of 20–60 °C, it is used to manufacture the inner and outer steel rings. On the inner lower end of the inner steel ring and the outer lower end of the outer steel ring, there is a circular silicone heating pad firmly attached to the steel rings, ensuring that the steel rings maintain the preset temperature during the heat transfer to the concrete and the heat dissipation to the surrounding air.

The procedures for forming the concrete specimen and the testing process are as follows:

Fig. 1. Schematic diagram of improved dual steel rings restraint test.

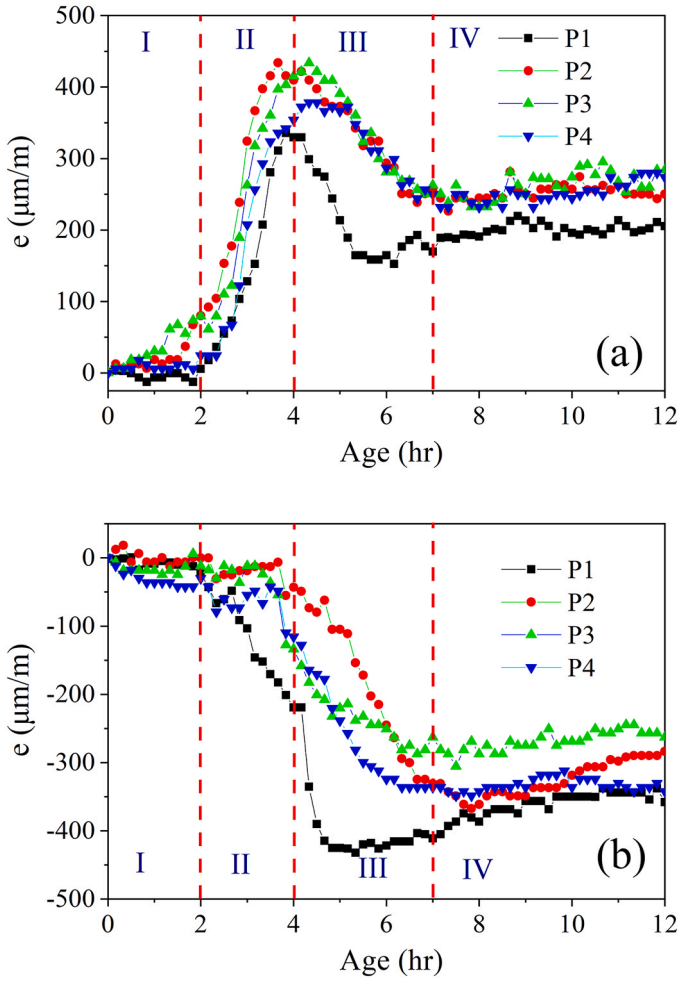

Fig. 2. Dual steel rings strain situation during the steam curing process: (a) the outside of the outer steel ring; (b) the inside of the inner steel ring.

(i) Place a plastic ring with a thickness of 2 mm on the base of the test mold (made of steel material and 8 mm thick) and on the inner side of the dual steel rings to prevent direct contact between the concrete specimen and the silicone heating equipment, which is positioned beneath the base of the mould.

(ii) Pour fresh concrete into the dual steel ring mold in two layers and place both the specimen and the mold on a vibration table for approximately 30 s to control the specimen's height to around 74 mm. After vibration, cover the surface of the specimen with a thin layer of plastic film and another plastic ring to prevent water evaporation from the specimen's surface, and then place the silicone heating equipment above the plastic ring.

(iii) Before the concrete specimen reaches the required setting time (setting time at least 3 hr), place the specimen and the mold in the test equipment. Install the eddy current sensors and calibrate the distances between each sensor and the inner wall of the inner steel ring and between each sensor and the outer wall of the outer steel ring, ensuring that the distances between 1.1 ~ 1.2 mm. When the test begins, activate both the upper and lower silicone heating equipment, heating the specimen from 20 ℃ to 60 ℃ within 2 hr, then maintaining constant temperature treatment at 60 ℃ for 8 hr before turning off the equipment to allow the specimen to cool naturally.

(iv) The acquisition frequency is once per minute, and the final result is the average of three specimens. The test results consist of the measured radial displacements of the dual steel rings, and the typical test results are presented in Fig. 4.

2.2. Internal stress calculation and test method validation

Since there is a correlation between the internal stress test method of steam-cured concrete and the stress analysis method of thick wall cylinder, the steel ring is taken as the object, and the steel ring microelement is illustrated in Fig. 5.

According to Fig. 5, there is

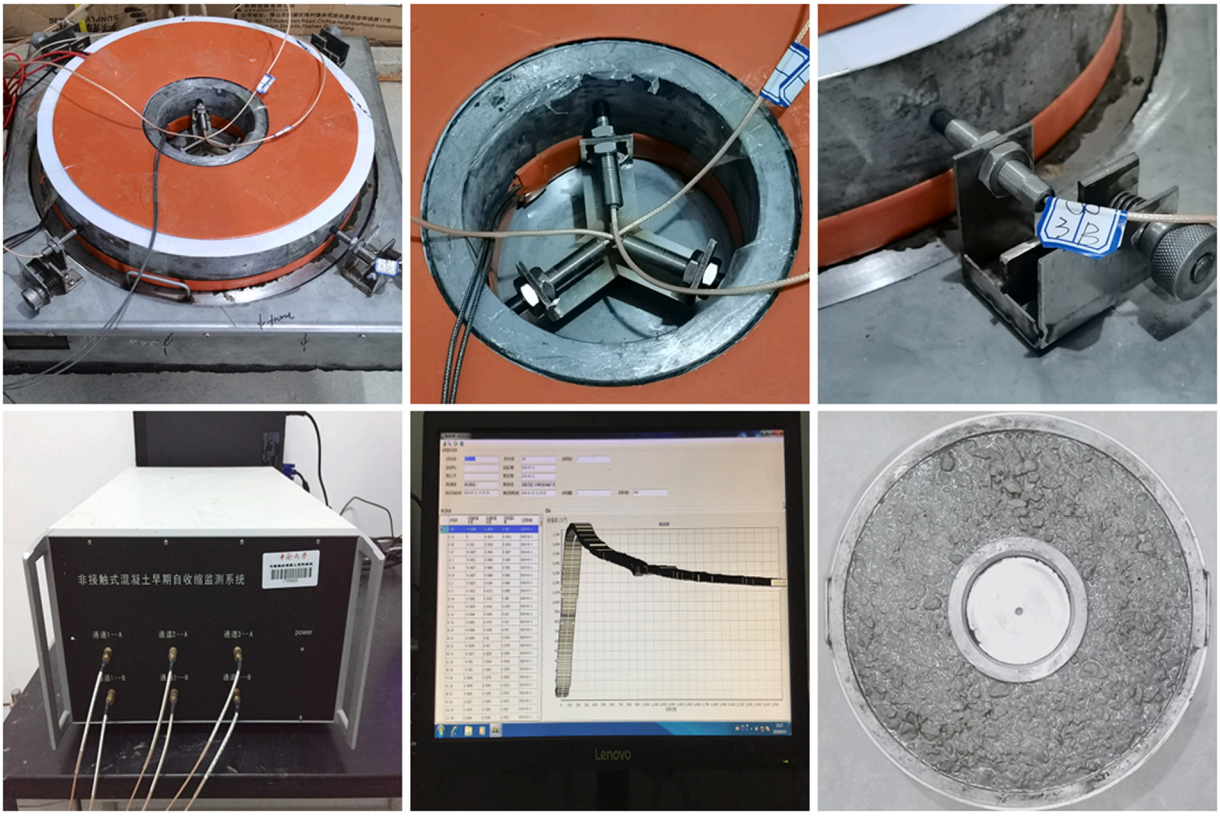

Fig. 3. Test diagram of dual steel rings test system and concrete specimen.

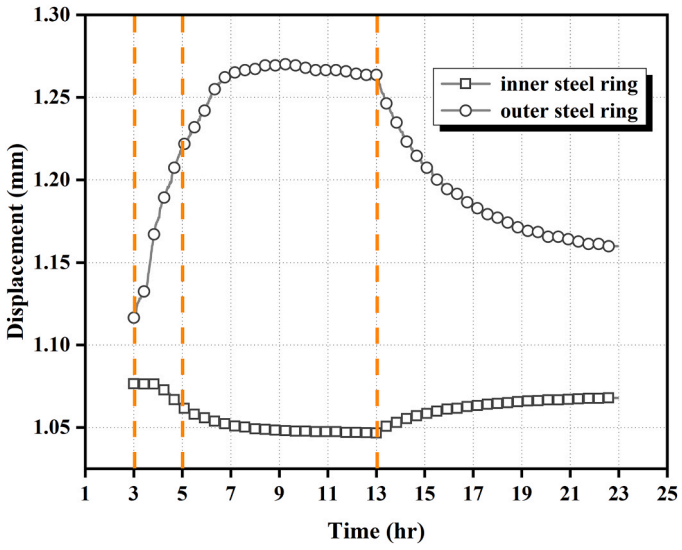

Fig. 4. Radial displacements diagram of dual steel rings.

$$\varepsilon_\theta = \frac{(r+w)\cdot \mathrm{d}\theta - r\cdot \mathrm{d}\theta}{r\cdot \mathrm{d}\theta} = \frac{w}{r} \tag{1}$$

where: r represents the inner diameter of the steel ring microelement, and w denotes the outward displacement of the inner side of the steel ring microelement. This means that changes in the radial length of the steel ring microelement can be directly converted into annular strain. The schematic diagram and device dimensions are illustrated in Fig. 6.

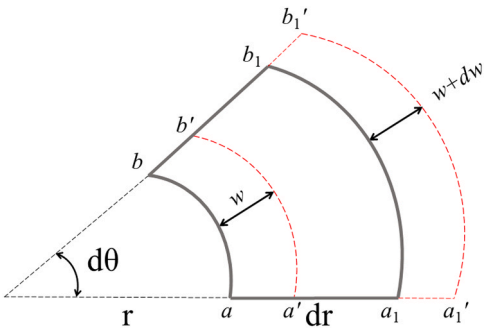

Fig. 5. Deformation of microelement of the steel ring.

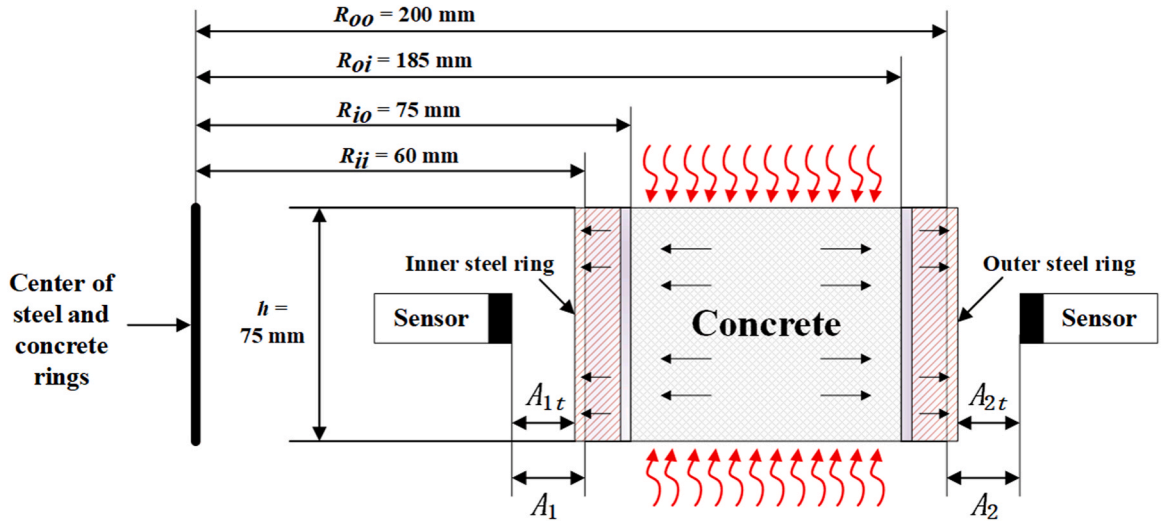

Fig. 6. Schematic diagram and dimensions of dual steel rings test mould.

Based on Fig. 6, it is evident that the radial displacement of the steel ring, as monitored by the eddy current sensor, can be transformed into the annular strain of each steel ring by using Eq. (2), which is as follows:

$$\begin{cases} \varepsilon_i = \dfrac{A_{1t} - A_1}{R_{ii}} \\ \varepsilon_o = \dfrac{A_2 - A_{2t}}{R_{oo}} \end{cases} \tag{2}$$

where: ε_i and ε_o are the strains generated by the inner and outer steel rings, respectively; A_{1t} and A_1 are the distances measured by the inner sensor at time t and the initial moment, respectively; A_{2t} and A_2 are the distances measured by the outer sensor at time t and the initial moment, respectively. Since the test system has 6-channel data samplers, there are

$$\begin{cases} \varepsilon_{ii} = \dfrac{\varepsilon_{i1} + \varepsilon_{i2} + \varepsilon_{i3}}{3} \\ \varepsilon_{oo} = \dfrac{\varepsilon_{o1} + \varepsilon_{o2} + \varepsilon_{o3}}{3} \end{cases} \tag{3}$$

where: ε_{i1}, ε_{i2}, and ε_{i3} are the inner ring strains measured by the three inner sensors, respectively; ε_{o1}, ε_{o2}, and ε_{o3} are the outer ring strains measured by the three outer sensors, respectively.

Meanwhile, in order to calculate the internal stress, the following reasonable assumptions need to be made [12]:

(i) The steel ring is in close contact with the concrete specimen, and the contact surface is fully adhered to prevent any relative slip deformation during the development of expansion or shrinkage of specimen.
(ii) The deformation of the outer wall of the steel ring and the deformation of the inner wall of the concrete occur simultaneously and have equal values.

(iii) The concrete specimen undergoes elastic deformation and creep, while the steel rings undergo only elastic deformation.
(iv) The deformation of the steel ring and the specimen is uniform in radial direction or along the ring.

It is well-established that the annular stress at any radius within the concrete ring can ultimately be calculated based on the radial stresses acting on the inner and outer steel rings [13–16], as follows:

$$\begin{cases} P_i = -\varepsilon_i \cdot E_s \cdot \left(\dfrac{R_{io}^2 - R_{ii}^2}{2R_{io}^2} \right) \\ P_o = \varepsilon_o \cdot E_s \cdot \left(\dfrac{R_{oo}^2 - R_{oi}^2}{2R_{oi}^2} \right) \\ \sigma_\theta = \dfrac{P_i \cdot R_{io}^2 - P_o \cdot R_{oi}^2}{R_{oi}^2 - R_{io}^2} + \dfrac{(P_i - P_o) \cdot R_{io}^2 \cdot R_{oi}^2}{R_{oi}^2 - R_{io}^2} \cdot \dfrac{1}{r^2} \end{cases} \tag{4}$$

where: P_i and P_o are the radial stresses of the concrete ring acting on the inner and outer steel rings, MPa, respectively; E_s is the modulus of elasticity of the steel ring, with a modulus of 210 GPa, and it varies very little within 100 ℃ range; σ_θ is the annular stress of the concrete ring with different radii inside the ring, MPa. The annular stress resembles a comprehensive force, encompassing the stress behaviors arising from internal factors during the curing process of fresh concrete, thus serving as a comprehensive representation.

The above formula is primarily derived from the stress analysis of thick-walled cylinders. r represents the radius of the concrete ring, which varies from 75 mm to 185 mm, allowing for characterization of the annular stresses at various radii. When the concrete specimen is in an expanded state, the calculation result can be manifested as compressive stress. Currently, the primary challenge lies in the unclear temperature gradient of concrete and the subsequent inaccurate calculation of its thermal elastic stress, which undoubtedly impacts the computed results. Therefore, the authors did not consider making corrections to the results for thermal elastic stress.

To achieve temperature compensation for the dual steel rings while processing the strain data of the rings and the specimen, the eddy current sensor and resistive strain gauge were employed for in-situ detection to monitor the strain of the empty dual steel rings during the thermal treatment period. Schematic diagram of contrast test and the results are presented in Figs. 7 and 8, respectively.

As seen in Fig. 8, the maximum strains recorded by the strain gauges for both the inner and outer steel rings were primarily around 400 $\mu\varepsilon$ during the initial thermal treatment. In this stage, the inner steel ring exhibited a compressive strain, while the outer steel ring showed tensile strain. However, by the end of the cooling phase, the residual strains of the inner steel ring and the outer steel had reduced to approximately 150 $\mu\varepsilon$ and 60 $\mu\varepsilon$, respectively. Subsequently, all the feedback data from the strain gauges were reset to zero, and then the second thermal treatment began. During this phase, the maximum strains for both the inner and outer steel rings, as monitored, were approximately 350 $\mu\varepsilon$ after entering the constant temperature curing stage. This represented a significant decrease compared to the first treatment.

Simultaneously, the strain gauges were unable to detect residual strains at the end of the cooling period, suggesting that the all gauges had undergone irreparable deformation during the initial thermal treatment. In the subsequent third treatment, the maximum strains in both the inner and outer steel rings showed a slight decrease, highlighting the lack of accuracy and reliability in the test data when using the same strain gauge under significant temperature variations and humidity. Meanwhile, the maximum strains monitored by the eddy current sensors for the inner and outer rings during all three thermal treatments remained at approximately 360 $\mu\varepsilon$. The temperature strains in both rings remained relatively stable throughout the heating, constant temperature curing, and cooling phases. This suggests that the non-contact method for monitoring strain changes during the non-steady state thermal treatment is more accurate.

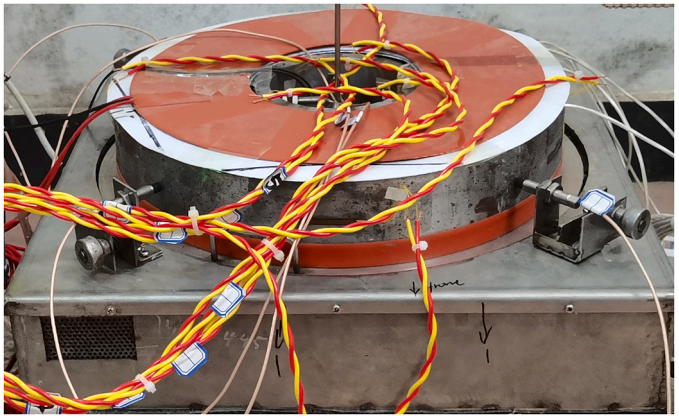

Fig. 7. Contrast test for measuring the strain of empty dual steel rings by strain gauge and non-contact methods.

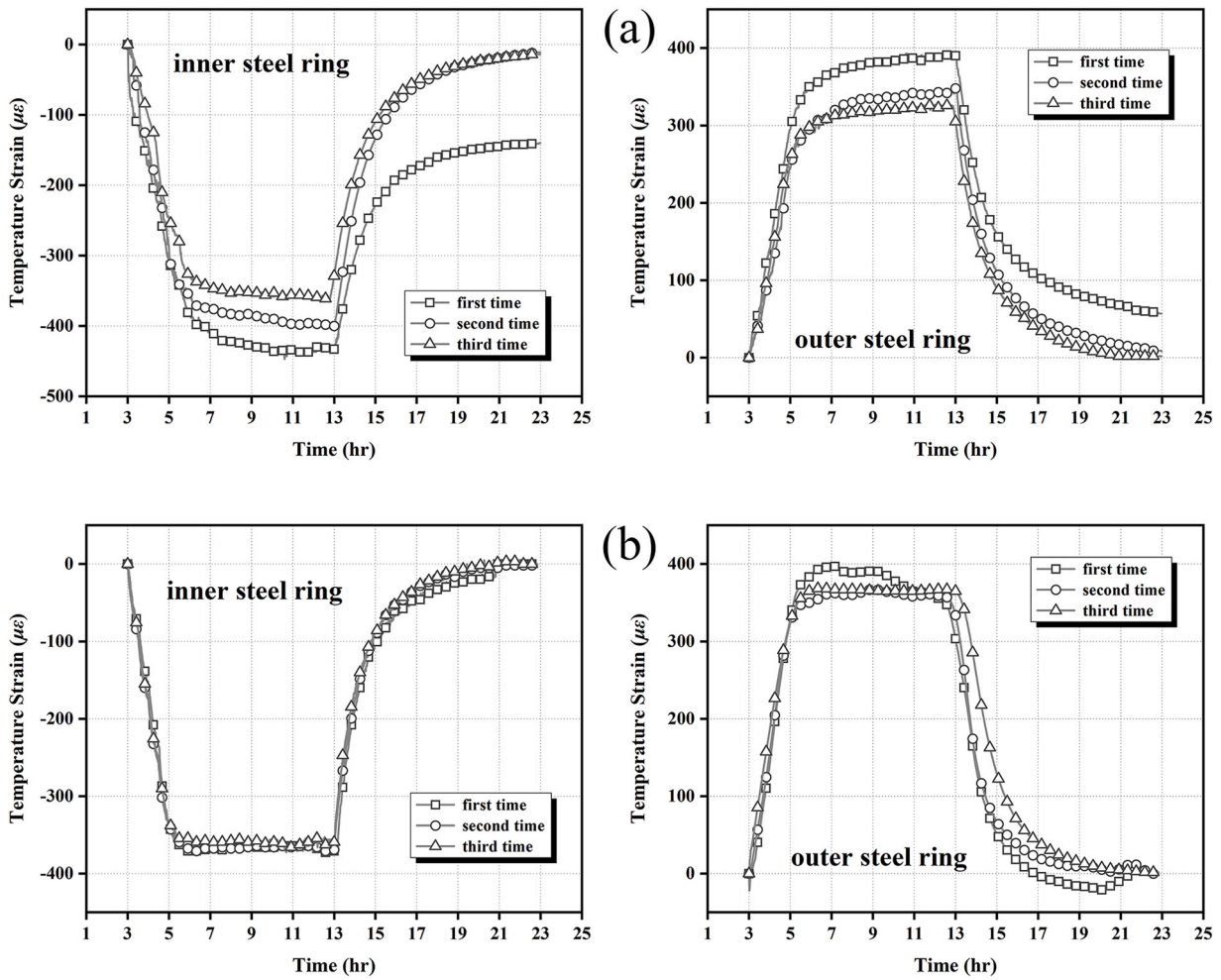

Fig. 8. Contrast test results of measured strain of empty dual steel rings: (a) strain gauge method; (b) non-contact method.

2.3. Raw materials and concrete mixing proportions

The 42.5 Portland cement (PC) produced by the China Building Materials Academy, without any additional blending materials is adopted. The technical specifications for PC are listed in both Table 1 and Table 2. The fine aggregate is Xiangjiang River sand (S) with a fineness modulus of 2.8. The coarse aggregate consisted of crushed limestone gravel (G) with particle sizes ranging from 5 mm to 20 mm. Within the coarse aggregate, 40 % is in the range of 5–10 mm, and 60 % is in the range of 10–20 mm. The mixing water (W) is ordinary tap water at room temperature (20 ℃). Additionally, the polycarboxylate high-performance water-reducing agent (SP, % by weight of cement) produced by Jiangsu Sobute New Materials Co., Ltd is used.

Because both the *w/c* and aggregate content of concrete have a certain influence on the early structural strength of concrete. As a result, the internal stress changes during the thermal treatment vary among different concrete mixtures. Five groups of steam-cured concrete mixing proportions were designed, which were presented in Table 3. The control group is represented by C1, and groups C1 to C3 were designed to assess the effects of initial free water content on internal stress. Additionally, groups C4 and C5 were designed to evaluate the impact of aggregate content on internal stress, with the sand ratio being the same as that of the control group C1. To ensure that each concrete group undergoes testing under consistent conditions with slump values ranging from 70 to 85 mm, various SP contents were employed.

Table 1
Main oxide composition of PC.

Cement	Oxide composition (%)						
	SiO_2	Al_2O_3	Fe_2O_3	CaO	MgO	SO_3	Na_2O_{eq}
PC	20.85	4.91	3.23	63.74	2.26	2.12	0.54

Table 2
Relative content of PC clinker (%).

Type	C_3S	C_2S	C_3A	C_4AF	Other
Ratio	57.83	15.77	7.69	11.03	7.68

Table 3
Mixing proportions of concrete for internal stress tests (kg/m^3).

Group	PC	S	G	W	SP	w/c	p/a
C1	450	660	1210	135	3.60	0.30	0.39
C2	440	647	1186	154	2.64	0.35	0.42
C3	433	635	1164	173	1.73	0.40	0.45
C4	497	636	1167	149	3.97	0.30	0.44
C5	413	679	1248	124	3.30	0.30	0.34

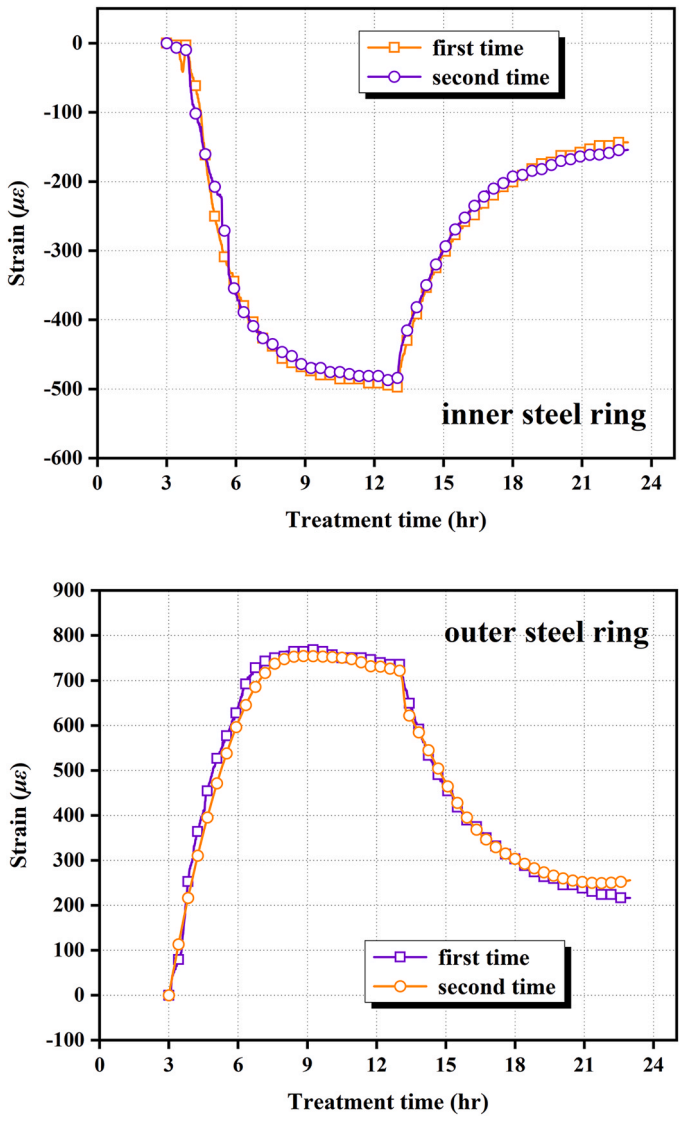

Fig. 9. Strains of group C1 on dual steel rings during the thermal treatment period.

3. Results and discussion

3.1. Characterization of internal stress evolution

The strains generated by group C1 on the dual steel rings during the thermal treatment are illustrated in Fig. 9.

As can be seen from Fig. 9, the effect of concrete on the strain of the inner and outer steel rings under thermal treatment condition is similar: the strain increases rapidly in the 3 hr ~ 5 hr of the heating stage. However, due to the influences of heat conduction and heat radiation, the internal temperature of the specimen rises more slowly, and the heat transferred to the concrete from the base of the mould and the steel rings gradually accumulates, which results in continued changes in the strain of the inner and outer steel rings. The strains of the inner and outer steel rings finally stabilize between 2 hr ~ 4 hr into the early constant temperature curing period. The strain of the inner ring remains within 500 $\mu\varepsilon$ in the middle and late stages of the constant temperature curing, while the strain of the outer ring reaches about 750 $\mu\varepsilon$, which is higher than that of the inner ring.

Then, both the inner and outer rings experience a rapid decrease in the early period of cooling, with the decreasing trend being smoother in the later stages. However, both exhibit unrecoverable residual strains, with the strain of the inner ring at about 150 $\mu\varepsilon$ at the end of the cooling period, and the outer ring reaching around 240 $\mu\varepsilon$, with the residual strain of the outer ring higher than that of the inner ring.

Furthermore, the impact of the control concrete on both the inner and outer rings in the two parallel tests is also similar, with very small strain differences between the two tests at the same moment, indicating good test method reproducibility. The internal stress of the control concrete at the radius r with 75 mm in the treatment process under restraint is calculated and displayed in Fig. 10.

As depicted in Fig. 10, during the thermal treatment, the internal stresses within the specimens predominantly exhibit compressive characteristics. This is attributed to the combined effect of the rings' constraints and the transition of the concrete from a plastic state to a certain degree of stiffness. Based on these two test results, the evolutionary patterns of internal stress can be summarized as follows:

(i) Compressive stress increases rapidly during the heating stage and eventually reaches about 14 MPa at the end of heating stage.
(ii) Compressive stress gradually decreases during the constant temperature curing period and reaches approximately 8 MPa at the end of this period.
(iii) There is a sharp decrease in compressive stress as cooling stage begins, followed by a slight recovery in the first 2 hr ~ 4 hr. This recovery is mainly due to differences in the heat dissipation efficiency between the steel rings and the concrete specimen. However, as the temperatures of both gradually approach each other and eventually reach room temperature, the compressive stress continues to decrease and eventually stabilizes. The residual internal stress of the control group at the end of the cooling period remains within 2 MPa under restraint.

Based on the aforementioned evolutionary characteristics, it is evident that the internal stress of thermally treated concrete is significantly elevated. This contrasts with the conventional understanding of concrete's early strength development. Several potential

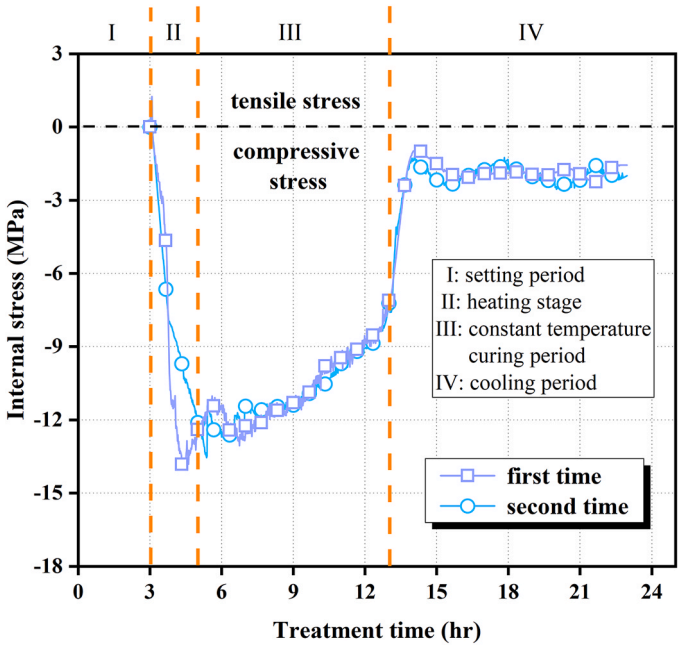

Fig. 10. Internal stress of the control group under restraint during the thermal treatment.

explanations for this phenomenon are considered below.

Firstly, fresh concrete undergoes a rapid stage of condensation and hardening during the heating phase. The concrete itself gradually transitions from a highly plastic state to a semi- plastic state and then to a state with a certain level of stiffness. Because the low modulus of elasticity and compressive strength of the specimen, coupled with the restraining effect of the inner and the outer steel rings, internal moisture expansion of concrete primarily contributes to the development of compressive stress [17] during this process.

Secondly, as the cement hydration process accelerates and the strength of the specimen rapidly during the constant temperature curing period [18], chemical shrinkage of the specimen and self-drying shrinkage caused by the chemical shrinkage gradually intensify [19]. This leads to the gradual development of internal shrinkage stress within the specimen. As the concrete structure becomes more refined and the moisture expansion effect diminishes, the shrinkage stress compensates for the compressive stress to some extent, resulting in a gradual reduction of compressive stress during this phase.

Finally, the internal stress of the specimen under restraint is manifested as residual compressive stress at the end of cooling period. This is mainly because the thermally treated concrete has completely hardened and gained high strength, and its expansion deformation that occurred during the heating stage cannot be fully recovered through the reduction of temperature-related deformation and the growth of shrinkage deformation [3,20,21]. Additionally, the inner and the outer steel rings also retract, creating a compressive tightening effect on the expanded concrete. Consequently, there are residual strains in both the steel rings, resulting in low compressive stress within the thermally treated concrete.

The above analysis is based on the annular stress of the thermally treated concrete ring near the outer side of the inner steel ring, while the radius r of the concrete ring ranging from 75 mm ~ 185 mm. As a result, the internal annular stresses of the concrete ring under restraint with different radii can be obtained, as shown in Fig. 11. The internal stresses at the end of the heating and cooling periods are shown in Table 4.

According to the Fig. 11, the internal annular stresses of the thermally treated specimen under restraint with different radii first peak at the end of heating stage. The peak internal stresses of the specimen exhibit a decreasing trend as the concrete ring from the inside to the outside. The peak internal stress of the specimen decreases to 5.82 MPa when r is 185 mm (the outside of the concrete ring), which is about 59 % less than that of the concrete ring at r with 75 mm. When r is lower than 85 mm, the internal stress can reach its peak at the end of heating stage. However, as r continues to increase, the peak internal stress at the end of heating stage decreases rapidly but then rises during the first 2 hr of the constant temperature curing period. This phenomenon is attributed to the slower temperature increase of the concrete. When the internal and external temperatures of the specimen gradually align with the thermal treatment environment, the strains of the inner and the outer rings will also reach their respective maximum value.

Secondly, the internal stresses of the concrete ring at different radii locations under restraint essentially remain constant at the end of constant temperature curing period, but the rate of decrease in these stresses varies significantly. One possible explanation is that when the thermal treatment reaches a certain point, the shrinkage deformation of the specimen is limited. As the radius of the concrete ring increases, the shrinkage stress at that radius decreases, resulting in a reduced compensatory effect for the internal compressive stress.

Finally, the internal stresses present an increase with the concrete ring radius from the inside to the outside, with the residual

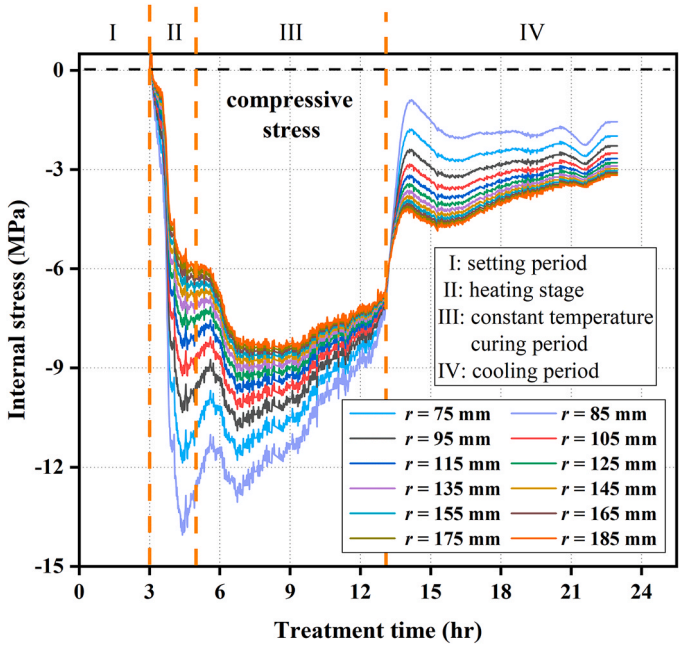

Fig. 11. Internal stresses of thermally treated control group specimen under restraint with different radii.

Table 4
Internal stress of thermally treated control group specimen under restraint at the ends of the heating and cooling periods.

r (mm)	Compressive stress (MPa)	
	at the end of heating	at the end of cooling
75	-14.05	-1.56
85	-11.87	-1.98
95	-10.34	-2.28
105	-9.23	-2.50
115	-8.39	-2.67
125	-7.75	-2.79
135	-7.25	-2.89
145	-6.84	-2.97
155	-6.51	-3.03
165	-6.24	-3.09
175	-6.02	-3.13
185	-5.82	-3.17

compressive stress at the outer edge of the concrete ring being approximately 103 % higher compared to the inner edge at the end of the cooling period. Simultaneously, the more noticeable decrease in internal stresses from the inside to the outside of the thermally treated concrete ring with different radial locations indicates that the outer part of the concrete, subject to the restraint by the steel rings, experiences greater effects. The peak internal compressive stresses and residual compressive stresses of fresh concrete under restraint with different radii positions during the thermal treatment period can be seen in Fig. 12. Furthermore, these phenomena can be better understood by analyzing the deformation patterns of the inner and outer steel rings and the concrete ring, as shown in Fig. 13.

As can be seen in Fig. 13, on the one hand, both the inner and the outer steel rings undergo thermal expansion deformations, D_{SRi} and D_{SRo}, respectively. Simultaneously, the concrete ring experiences thermal expansion deformations, D_{Ci} and D_{Co}, which exert pressure on the inner and the outer steel rings during the heating stage. When r is 75 mm, the significant moisture expansion of the concrete ring acts on the outside of the inner steel ring, causing the inner steel ring to expand outward. Consequently, the concrete ring experiences stronger restraint at this location, resulting in a smaller expansion strain of the inner steel ring and higher peak internal compressive stress. When r is 185 mm, the moisture expansion of the concrete ring impacts on the inside of the outer steel ring. Both the outer steel ring and the concrete ring expand outward, leading to a greater expansion strain in the outer steel ring compared to the inner steel ring. Furthermore, due to the simultaneous expansion of the outer steel ring and the concrete ring, the restraint of the concrete ring at this position is reduced, resulting in a lower peak compressive stress within the concrete ring.

On the other hand, both the inner and the outer steel rings experience inward shrinkage deformations, D_{SRi}' and D_{SRo}', respectively. Simultaneously, the concrete ring will also undergo shrinkage deformations, D_{Ci}' and D_{Co}', which exert pressure on the inner and the outer steel rings during the cooling period. When r is 75 mm, the concrete already possesses high strength, causing the specimen and the inner steel ring shrinks inwards. This implies that the concrete experiences the least restraint at this position, resulting in the lowest residual compressive stress. However, when r is 185 mm, the shrinkage deformation cannot fully offset the significant expansion deformation of the specimen. Moreover, the outer steel ring further contracts inwards, intensifying the restraining effect on the concrete ring at this position. Consequently, the residual strain of the outer steel ring is the largest, leading to an increase in residual compressive stress. This demonstrates that the internal stress of thermally treated concrete can reach such levels under the restraint of both the inner and the outer steel rings, as well as the inherent restraint of the concrete itself.

For ease of analysis, all calculations related to internal stress in thermally treated concrete under restraint are conducted at a radius of 75 mm. In other words, this paper focuses on discussing the internal stress within the concrete ring at the smallest radius.

3.2. Influence of w/c on internal stress

The results of internal stress tests of fresh concrete under restraint with varying free water content during the thermal treatment period are illustrated in Fig. 14.

As depicted in Fig. 14, the peak internal stress of group C1 is around 14 MPa. With an increase of w/c, the peak internal stresses of groups C2 and C3 increase by 14.3 % and 35.7 %, reaching 16 MPa and 19 MPa, respectively.

Firstly, the rapid increase in internal stresses during the heating stage is primarily due to the intense expansion of different constituent materials inside fresh concrete and the uneven heating of the concrete in the non-steady-state treatment environment. A significant residual expansion pressure acts on the outside of the inner steel ring, which can increase with higher moisture content in the system.

Secondly, the decreasing trend of internal stress in concrete is significant. The decrease in internal stress for group C1 is 49.5 %, and for group C3, it's 47.4 % during the constant temperature curing stage. This decrease occurs mainly because the steel rings and concrete ring gradually reach the same temperature when the maintenance temperature stabilizes. As a result, the thermal expansion effect of concrete ring decreases, while self-drying and chemical shrinkages gradually manifest. A higher w/c provides more free water inside the system, which exacerbates the shrinkage deformation of the specimen during the constant temperature curing period. The gradual increase in the internal shrinkage stress in the concrete compensates for parts of the compressive stress, ultimately leading to

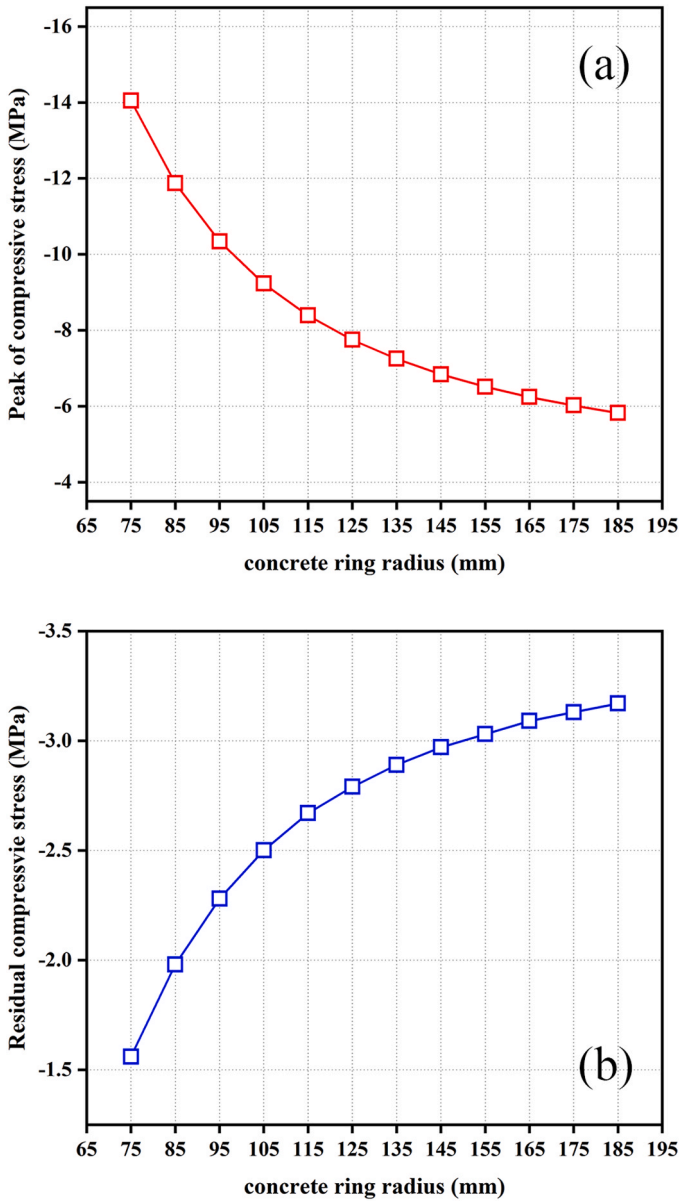

Fig. 12. Peak internal compressive stress and residual compressive stress of thermally treated concrete under restraint with different radii position: (a) at the end of heating; (b) at the end of cooling.

an overall reduction in the internal stress of the specimen.

Subsequently, the internal stress of thermally treated concrete decreases rapidly in the first 2 hr, mainly due to the rapid decrease in the overall system temperature, and the residual expansion pressure inside the concrete is diminishes, resulting in a rapid decrease in internal stress upon entering the cooling period.

Finally, the internal residual compressive stress of thermally treated concrete under restraint with different w/c falls within the range of 1 MPa ~ 3 MPa.

3.3. Influence of p/a on internal stress

The results of internal stress tests of fresh concrete under restraint with varying aggregate content during the thermal treatment period are illustrated in Fig. 15.

As shown in Fig. 15, the trends in changing internal stresses for groups C1, C4, and C5 are essentially the same as those observed for groups C1 ~ C3 under the restraint of dual steel rings. The peak internal stress for group C4 is approximately 20 MPa. However, with a decrease in p/c, the internal stresses of groups C1 and C5 decrease by about 30 % and 50 %, respectively, when compared to that of

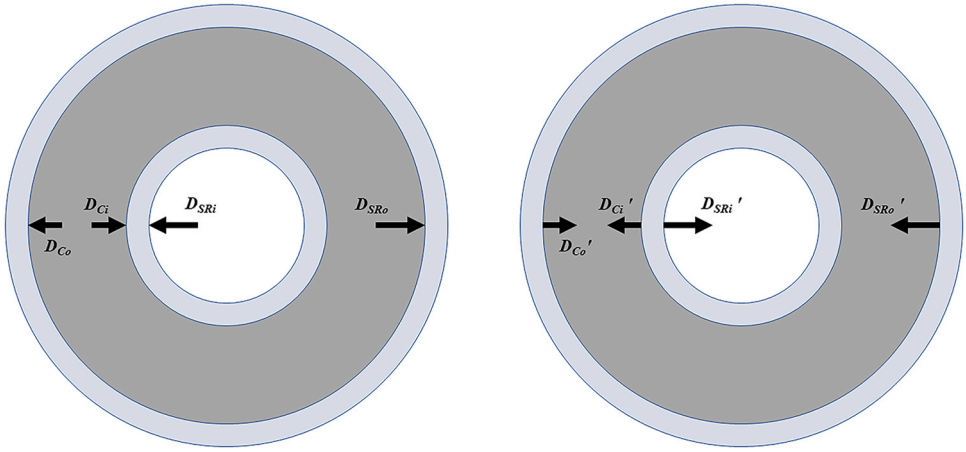

Fig. 13. Deformation diagram of dual steel rings and concrete ring during the thermal treatment period: (a) during the heating stage; (b) during the cooling period.

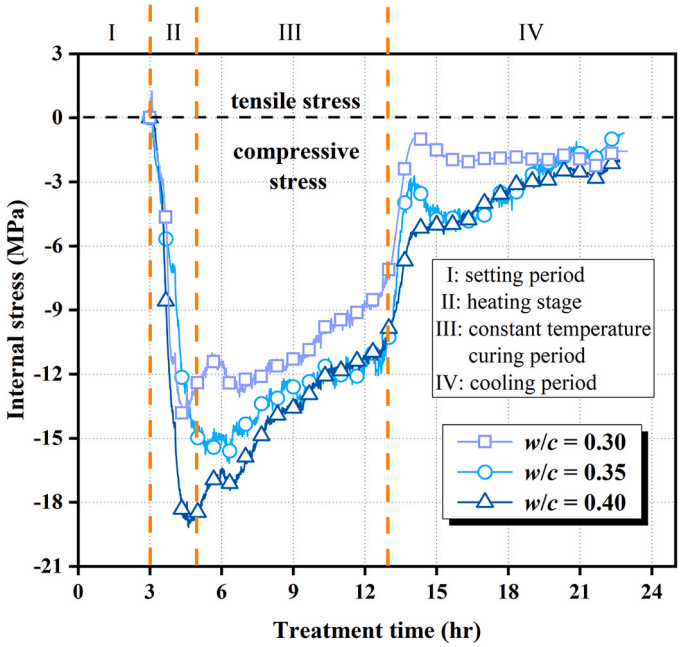

Fig. 14. Internal stress test results of concrete under restraint during the thermal treatment period with different *w/c*.

group C4. It is evident that increasing the aggregate content in concrete effectively controls the internal stress of fresh concrete under restraint during the thermal treatment period.

Firstly, the primary reason for the rapid increase in internal stresses during the heating stage remains formation of a significant residual expansion pressure inside the concrete, which is inevitable when utilizing steam curing or thermal treatment.

Secondly, the internal stress of concrete with different *p/a* decreases significantly during the constant temperature stage. In the case of group C4, there is a remarkable reduction of 66.7 %. As the aggregate content in the concrete decreases, the constraining effect on the expansion and shrinkage deformation of the specimen diminishes substantially, and the concrete becomes porous, which hampers the dissipation of the internal stress.

Consequently, the concrete undergoes considerable volume deformation under the non-steady state humidity-and-heat environment. In contrast, the internal stress of group C5 remains relatively stable when compared to that of group C4, indicating that raising the aggregate content in fresh concrete under a consistent sand ratio has a positive effect on densifying the concrete structure and enhancing its ability to withstand and transfer forces.

Finally, the decreasing trends of internal stress in different concrete mixes follow a similar pattern to those with varying *w/c*. The internal stress decreases rapidly within the first 2 hr and exhibits slight increase in the subsequent 2 ~ 4 hr after entering the cooling

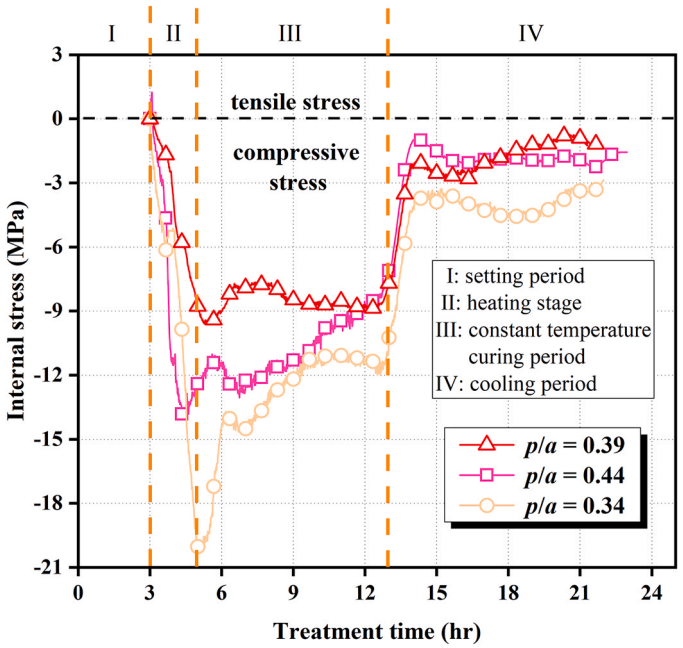

Fig. 15. Internal stress test results of concrete under restraint during the thermal treatment period with different *p/a*.

period. Consequently, the internal residual compressive stresses of groups C1 and C5 range from 1 ~ 2 MPa, while that of group C4 remains around 3 MPa.

Clearly, a significant residual stress is present within steam-cured or thermally treated fresh concretes. This stress invariably exerts an adverse influence on both the microscopic and macroscopic structure and properties of the concrete, resulting in a weakening of its mechanical and durability performance. This factor contributes to the development of thermal damage in steam-cured concrete.

4. Conclusions

The process of thermal treatment generates substantial internal stress in fresh concrete under the restraint of dual steel rings. This paper outlines the testing device and method for internal stress, and elaborates on the evolution characteristics of thermally treated concrete, leading to the following conclusions:

(i) The inner steel ring experiences compressive strain, while the outer steel ring undergoes tensile strain. Both reach their maximum values when the concrete acts on them at the end of heating stage.
(ii) The internal stresses in thermally treated concrete under restraint are predominantly compressive. They exhibit a rapid increase during the heating stage, followed by a gradual decline in the constant temperature curing stage and a further reduction during the cooling period with a slower downward trend.
(iii) Both *w/c* and *p/a* have a significant impact on the internal stress of thermally treated concrete under the effect of dual steel rings. Without considering thermal elastic stress, the peak internal stress in the concrete with 0.3 *w/c* is 14 MPa, whereas it reaches 19 MPa ~ 20 MPa for concrete with 0.4 *w/c* or 0.44 *p/a*.
(iv) Control over the internal stress in steam-cured or thermally treated concretes under restraint can be achieved by reducing the initial free water content and raising the initial structural strength of the concrete. For example, by using rapid-setting cement, nanoscale particle materials, water-absorbing resins, reducing the water-to-cement ratio, or employing designed aggregate gradation, and so on.

Declaration of Competing Interest

The authors declare that they have no known competing financial interests or personal relationships that could have appeared to influence the work reported in this paper.

Data Availability

Data will be made available on request.

Acknowledgements

This work was supported by Hunan Provincial Natural Science Foundation [grant number 2023JJ40753] and the Postdoctoral Science Foundation of Central South University [grant number 140050039].

References

[1] Y. Xiang, Y. Xie, G. Long, et al., Residual expansion deformation of high-speed railway steam-cured concrete: mechanism, modeling, and measurement, Arch. Civ. Mech. Eng. 21 (2021), 138, https://doi.org/10.1007/s43452-021-00281-9.
[2] X. Han, H. Fu, G. Li, et al., Volume deformation of steam-cured concrete with slag during and after steam curing, Materials 14 (2021) 1647, https://doi.org/10.3390/ma14071647.
[3] Y. Xiang, Y. Xie, G. Long, Volume deformation characteristics of concrete mixture during thermal curing process, Int. Conf. Mater. Sci. Manuf. Eng. Paris 253 (2019) 01008, https://doi.org/10.1051/matecconf/201925301008.
[4] J. Shi, B. Liu, S. Shen, et al., Effect of curing regime on long-term mechanical strength and transport properties of steam-cured concrete, Constr. Build. Mater. 255 (2020), 119407, https://doi.org/10.1016/j.conbuildmat.2020.119407.
[5] J. Shi, B. Liu, X. Wu, et al., Effect of steam curing on surface permeability of concrete: Multiple transmission media, J. Build. Eng. 32 (2020), https://doi.org/10.1016/j.jobe.2020.101475.
[6] C. Zou, G. Long, Y. Xie, et al., Evolution of multi-scale pore structure of concrete during steam-curing process, Microporous Mesoporous Mater. 288 (2019), 109566, https://doi.org/10.1016/j.micromeso.2019.109566.
[7] Y. Xiang, G. Long, Y. Xie, et al., Thermal damage and its controlling methods of high-speed railway steam-cured concrete: a review, Struct. Concr. 22 (S1) (2020) E1074–E1092, https://doi.org/10.1002/suco.202000433.
[8] M. Wang, Y. Xie, G. Long, et al., The impact mechanical characteristics of steam-cured concrete under different curing temperature conditions, Constr. Build. Mater. 241 (2020), 118042, https://doi.org/10.1016/j.conbuildmat.2020.118042.
[9] Q. Xia, H. Li, A. Lu, et al., Restrained stress and creep behavior of mortar with expansive agent at early ages (in Chinese), J. Chin. Ceram. Soc. 44 (11) (2016) 1602–1608, https://doi.org/10.14062/j.issn.0454-5648.2016.11.09.
[10] He J. and Ma K. Early age stress development of steam-curing pastes restrained by dual rings. The 12th International Symposium on High Performance Concrete, Chengdu, 2017, 132–133. (in Chinese). ⟨https://d.wanfangdata.com.cn/conference/ChZDb25mZXJlbmNlTmV3UzIwMjMwODMwEggxMDU5NjQ4OBoIcWR5enJ5YnM%3D⟩.
[11] Xie Y., Xiang Y., Long G., et al. Hydrothermal curing and its stress-strain integrated testing device and method for concrete. (Chinese Patent). ZL 2020 1 0798660.4, 2021. (in Chinese). ⟨https://d.wanfangdata.com.cn/patent/ChJQYXRlbnROZXdTMjAyMzA4MDcSE0NOMjAyMDEwNzk4NjYwLjRfc3EaCDF3dDhmcnRl⟩.
[12] G. Wang, J. Liu, J. Zheng, Study on the stress relaxation properties induced in restrained autogenous shrinkage of self-compacting concrete (in Chinese), J. Disaster Prev. Mitig. Eng. 39 (01) (2019) 82–88, https://doi.org/10.13409/j.cnki.jdpme.2019.01.012.
[13] D.P. Bentz, T.E. Nantung, W.J. Weiss, A dual concentric ring test for evaluating residual stress development due to restrained volume change, J. ASTM Int. 7 (09) (2010) 1–21, https://doi.org/10.1520/JAI103118.
[14] Q. Xia, H. Li, T. Yao, et al., Cracking behaviour of restrained cementitious materials with expansive agent by comprehensive analysis of residual stress and acoustic emission signals, Adv. Cem. Res. 29 (02) (2017) 81–90, https://doi.org/10.1680/jadcr.16.00111.
[15] J.L. Schlitter, D.P. Bentz, W.J. Weiss, Quantifying stress development and remaining stress capacity in restrained, internally cured mortars, Acids Mater. J. 110 (01) (2013) 3–11. ⟨https://www.nstl.gov.cn/paper_detail.html?id=9c7f459383dfb38f8b07b2b64c873735⟩.
[16] D. Zou, J. Weiss, Early age cracking behavior of internally cured mortar restrained by dual rings with different thickness, Constr. Build. Mater. 66 (2014) 146–153, https://doi.org/10.1016/j.conbuildmat.2014.05.032.
[17] He Z. Heat damage effects of steam curing on concrete and corresponding improvement measures. (Dissertation for the Doctoral Degree). Changsha: Central South University, 2012. (in Chinese). ⟨http://d.wanfangdata.com.cn/thesis/Y2426728⟩.
[18] X. Zhao, B. Liu, N. Jiang, Effect of the steam curing parameters on the hydration characteristics of hardened cement paste (. (in Chinese)), Concrete 246 (2010) 28–30, https://doi.org/10.3969/j.issn.1002-3550.2010.04.009.
[19] S. Kang, S. Hong, J. Moon, Shrinkage characteristics of heat-treated ultra-high performance concrete and its mitigation using superabsorbent polymer based internal curing method, Cem. Concr. Compos. 89 (2018) 130–138, https://doi.org/10.1016/j.cemconcomp.2018.03.003.
[20] L. Li, G. Long, F. Liu, et al., Deformation behavior of concrete during steam curing (in Chinese), Mater. Rep. 33 (04) (2019) 1322–1327, https://doi.org/10.11896/cldb.17120058.
[21] He Z., Long G., Xie Y., et al. Expansive deformation behavior of steam-cured cementitious materials and corresponding control measurement. Journal of Central South University, 2012, 43(05): 1947–1953. (in Chinese). ⟨http://www.wanfangdata.com.cn/details/detail.do?_type=perio&id=zngydxxb201205052⟩.